Inorg. Chem. **2003**, *42*, 4308–4315

Wavelength-Dependent Photofragmentation and Photoionization of Gaseous (η^4-Cycloocta-1,5-diene)(η^5-cyclopentadienyl)cobalt

Daniel Byun and Jeffrey I. Zink*

Department of Chemistry and Biochemistry, University of California at Los Angeles, Los Angeles, California 90095

Received February 6, 2003

Gas-phase photoreactions and photoproducts of the mixed-ligand compound (η^4-cycloocta-1,5-diene)(η^5-cyclopentadienyl)cobalt are reported. Significant amounts of the monoligated complexes CoCOD and CoCp are produced, and the relative amounts are wavelength dependent. The COD ligand (with the weakest metal–ligand bonds) is always preferentially labilized as expected, but the relative amounts of the CoCOD and CoCp fragments change by 1 order of magnitude as the excitation wavelength is changed. The gas-phase photoreactions exhibit other surprising features that are uncommon in the photoreactions of organometallic compounds in the gas phase. Significant amounts of the intact cation are formed, in contrast to most reported reactions where fragmentation of the weak metal–ligand bonds precedes ionization. Most surprisingly, fragmentation of the ligands occurs while the ligands are still coordinated. The resulting metal complexes contain ligand fragments that remain coordinated to the metal. Breaking several carbon–carbon bonds with retention of weaker metal–ligand bonds is unexpected. For example, C_5H_5 undergoes fragmentation while still coordinated to the cobalt, yielding smaller compounds such as $Co(CH)^+$, $Co(C_2H_2)^+$, $Co(C_3H_3)^+$, and $Co(C_4H_6)^+$. Correspondingly, coordinated COD yields $Co(C_6H_6)^+$, $Co(C_5H_5)^+$, $Co(C_4H_6)^+$, $Co(C_3H_3)^+$, $Co(C_2H_2)^+$, and $Co(CH)^+$. The wavelength dependence of the ligand labilization is examined by utilizing mass-selected resonance enhanced multiphoton ionization spectroscopy. Both broad bands and sharp lines are observed in the mass-selected excitation spectra. The action spectra obtained in the gas phase while monitoring the cobalt ion follow the absorption onset found in solution. The changes in fragmentation pathways are interpreted in terms of the initially accessed excited state.

Introduction

Gas-phase photochemical reactions of organometallic compounds and transition-metal coordination compounds are attracting interest because of their importance in understanding laser-assisted chemical vapor deposition.[1−9] The most thoroughly studied gas-phase photochemical reactions have been those of metal carbonyl compounds; sequential loss of the CO ligands leading to the production of metal ions is usually observed.[10−17] Metallocenes have also been well studied, and again photodecomposition to produce the bare metal ion is usually the most important process.[18−29] These studies show the explosive nature of photoexcitation in metal-

* To whom correspondence should be addressed. E-mail: zink@chem.ucla.edu.

(1) Baum, T. H.; Commita, P. B. *Thin Solid Films* **1992**, *218*, 80−94.
(2) Ehrlich, D. J.; Osgood, R. M., Jr.; Deutsch, T. F. *IEEE J. Quantum Electron.* **1980**, *QE16*, 1233−1243.
(3) Osgood, R. M.; Deutsch, T. F. *Science* **1985**, *227*, 709−714.
(4) Osgood, R. M., Jr. *Annu. Rev. Phys. Chem.* **1983**, *34*, 77−101.
(5) Eden, J. G. *Photochemical Vapor Deposition*; Wiley: New York, 1992.
(6) Hitchman, M. L.; Jensen, K. F. *Chemical Vapor Deposition: Principles and Applications*; Academic Press: San Diego, CA, 1993.
(7) Kodas, T. T.; Hampden-Smith, M. J. *The Chemistry of Metal CVD*; Wiley: Weinheim, Germany, New York, 1994.
(8) Cheon, J.; Zink, J. I. *J. Am. Chem. Soc.* **1997**, *119*, 3838−3839.
(9) Cheon, J.; Talaga, D. S.; Zink, J. I. *Chem. Mater.* **1997**, *9*, 1208−1212.
(10) Ashfold, M. N. R.; Howe, J. D. *Annu. Rev. Phys. Chem.* **1994**, *45*, 57−82.
(11) Boesl, U.; Neusser, H. J.; Schlag, E. W. *Chem. Phys. Lett.* **1982**, *87*, 1−5.
(12) Johnson, P. M. *Acc. Chem. Res.* **1980**, *13*, 20−26.
(13) Jackson, R. L. *Acc. Chem. Res.* **1992**, *25*, 581−586.
(14) Schlag, E. W.; Neusser, H. J. *Acc. Chem. Res.* **1983**, *16*, 355−360.
(15) Karny, Z.; Naaman, R.; Zare, R. N. *Chem. Phys. Lett.* **1978**, *59*, 33−37.
(16) Dietz, T. G.; Duncan, M. A.; Liverman, M. G.; Smalley, R. E. *J. Chem. Phys.* **1980**, *73*, 4816−4821.
(17) Smalley, R. E.; Wharton, L.; Levy, D. H. *Acc. Chem. Res.* **1977**, *10*, 139−145.
(18) Bar, R.; Heinis, T.; Nager, C.; Jungen, M. *Chem. Phys. Lett.* **1982**, *91*, 440−442.
(19) Engelking, P. C. *Chem. Phys. Lett.* **1980**, *74*, 207−210.

10.1021/ic0300518 CCC: $25.00
Published on Web 06/13/2003

containing compounds resulting in breaking of the relatively weak metal−ligand bonds, the complete loss of the ligands, and formation of the bare metal ion. Photoionization of the parent compound is usually a minor process, if it is observed at all, because fragmentation usually occurs before ionization. Fragmentation of the coordinated ligand to produce smaller coordinated fragments is not observed.

Recent studies in our laboratory on volatile metal-containing CVD precursors showed that relatively stable metal-containing photofragments can be produced by fragmentation of coordinated ligands.[30−39] When the desired deposit is a pure metal, ligand dissociation reactions leading to complete loss of the organic functionalities are desirable and metal species containing heteroatoms are undesirable. For example, photolysis of metal hexafluoroacetylacetonato compounds produces MF and MC diatomic fragments[35,38−40] and photolysis of methyl vinyl ketone complexes produces MO diatomic fragments.[37] The heteroatom is undesirable because it can contaminate the metal deposit. On the other hand, diatomic fragment production may be desirable when binary deposits are targeted. For example, metal amide compounds produce MN diatomic fragments upon photolysis, a desirable path when the target is a MN film such as TiN.[30] Our studies also show that the initially accessed excited state plays a significant role in influencing the relative concentrations of photoproducts. Studies on $Pd(hfac)_2$ and chromocene show that the photoproduction of certain photofragments is correlated with the originally accessed excited state and is a function of both excitation wavelength and laser fluence.[36]

It is of interest to determine if there is a wavelength dependence on relative ligand labilization and on the composition of metal-containing fragments in mixed-ligand compounds. To search for such effects, we examined the gas phase photochemistry of a cobalt compound with two different hydrocarbon ligands, η^4-cycloocta-1,5-diene, COD, and η^5-cyclopentadienyl, Cp, in the compound CpCoCOD. Molecules of this general type that contain both cyclopentadiene and alkene ligands have been used as precursors for conventional (thermally driven) chemical vapor deposition.[41−43] $CpM(C_2H_4)_2$ (M = Rh and Ir) were used as precursors for the deposition of pure rhodium and iridium films using laser-assisted chemical vapor deposition (LCVD) methods.[41] The bidentate alkene ligand cycloocta-1,5-diene provides greater thermal stability than η^2-alkene molecules and was chosen for this study of a mixed-ligand organometallic compound.

In this paper we report three surprising features in the photofragmentation reactions of CpCoCOD that are uncommon in the photoreactions of organometallic compounds in the gas phase. First, significant amounts of the intact cation are formed. Second, significant amounts of the monoligated complexes CoCOD and CoCp are produced and the relative amounts are wavelength dependent. The COD ligand (with the weakest metal−ligand bond) is always preferentially labilized as expected, but the relative amounts of the CoCOD and CoCp fragments change by 1 order of magnitude as the excitation wavelength is changed. Third, fragmentation of the ligands occurs while the ligands are still coordinated giving rise to photoproducts containing fragments of the original ligand that remain coordinated to the metal.

Experimental Section

1. Materials. CpCoCOD was prepared by literature methods[44] and purified by chromatography on neutral activated alumina with hexane as the eluent.

2. Spectroscopy. The time-of-flight mass spectrometer was constructed at UCLA on the basis of a design in the literature.[45,46] The photoionization for mass spectroscopy is carried out in a stainless steel cube (30 cm edge length) with quartz windows evacuated to less than 10^{-6} Torr with a 6 in. diffusion pump fitted with a water-cooled baffle. The sample is sublimed at 95 °C before it is seeded in He with a backing pressure of about 10^3 Torr. The precursor is admitted to the high-vacuum chamber via a supersonic jet. A General Valve series 9 high-speed solenoid valve (0.5 mm orifice) sends a 0.2 ms pulse of the sample into the chamber to intersect the incoming photons at 90°. An optical parametric oscillator (OPOTEK) pumped by the third harmonic of a Nd:YAG laser produces the photons within the 410−500 nm range (∼20 mJ/pulse, 0.5−1 nm line width, ∼10 ns pulse width) used for excitation. The beam diameter at the sample is about 1 mm. The energy range is scanned with a stepping motor driven micrometer

(20) Leutwyler, S.; Even, U.; Jortner, J. *Chem. Phys. Lett.* **1980**, *74*, 11−14.
(21) Leutwyler, S.; Even, U.; Jortner, J. *Chem. Phys.* **1981**, *58*, 409−421.
(22) Leutwyler, S.; Even, U.; Jortner, J. *J. Phys. Chem.* **1981**, *85*, 3026−3029.
(23) Liou, H. T.; Engelking, P. C.; Ono, Y.; Moseley, J. T. *J. Phys. Chem.* **1986**, *90*, 2892−2896.
(24) Liou, H. T.; Ono, Y.; Engelking, P. C.; Moseley, J. T. *J. Phys. Chem.* **1986**, *90*, 2888−2892.
(25) Nagano, Y.; Achiba, Y.; Kimura, K. *J. Phys. Chem.* **1986**, *90*, 1288−1293.
(26) Niles, S.; Prinslow, D. A.; Wight, C. A.; Armentrout, P. B. *J. Chem. Phys.* **1992**, *97*, 3115−3125.
(27) Ray, U.; Hou, H. Q.; Zhang, Z.; Schwarz, W.; Vernon, M. *J. Chem. Phys.* **1989**, *90*, 4248−4257.
(28) Opitz, J.; Harter, P. *Int. J. Mass Spectrom. Ion Processes* **1992**, *121*, 183−199.
(29) Tyndall, G. W.; Larson, C. E.; Jackson, R. L. *J. Phys. Chem.* **1989**, *93*, 5508−5515.
(30) Cheon, J.; Guile, M.; Muraoka, P.; Zink, J. I. *Inorg. Chem.* **1999**, *38*, 2238−2239.
(31) Cheon, J.; Zink, J. I. *Inorg. Chem.* **2000**, *39*, 433−436.
(32) Cheon, J.; Muraoka, P.; Zink, J. I. *Chem. Mater.* **2000**, *12*, 511−516.
(33) Cheon, J.; Kang, H.-K.; Zink, J. I. *Coord. Chem. Rev.* **2000**, *200−202*, 1009−1032.
(34) Muraoka, P.; Bitner, T. W.; Zink, J. I. *Res. Chem. Intermed.* **2000**, *26*, 69−84.
(35) Muraoka, P.; Byun, D.; Zink, J. I. *Coord. Chem. Rev.* **2000**, *208*, 193−211.
(36) Muraoka, P. T.; Byun, D.; Zink, J. I. *J. Phys. Chem. A* **2001**, *105*, 8665−8671.
(37) Bitner, T. W.; Zink, J. I. *Inorg. Chem.* **2002**, *41*, 967−972.
(38) Talaga, D. S.; Zink, J. I. *Inorg. Chem.* **1996**, *35*, 5050−5054.
(39) Talaga, D. S.; Hanna, S. D.; Zink, J. I. *Inorg. Chem.* **1998**, *37*, 2880−2887.
(40) Muraoka, P.; Byun, D.; Zink, J. I. *J. Am. Chem. Soc.* **2000**, *122*, 1227−1228.
(41) Cohan, J. S.; Yuan, H.; Williams, R. S.; Zink, J. I. *Appl. Phys. Lett.* **1992**, *60*, 1402.
(42) Chen, Y. J.; Kaesz, H. D.; Thridandam, H.; Hicks, R. F. *Appl. Phys. Lett.* **1988**, *53*, 1591−1592.
(43) Kaesz, H. D.; Silliams, R. S.; Hicks, R. F.; Zink, J. I.; Chen, Y. J.; Muller, H. J.; Xue, Z.; Xu, D.; Shuh, D. K.; Kim, Y. K. *New J. Chem.* **1990**, *14*, 527.
(44) Bonnemann, H.; Bogdanovic, B.; Brinkman, R.; He, D.-w.; Spliethoff, B. *Angew. Chem., Int. Ed. Engl.* **1983**, *22*, 728.
(45) Wiley: W. C.; McLaren, I. H. *Rev. Sci. Instrum.* **1955**, *26*, 1150−1157.
(46) Lubman, D. M.; Jordan, R. M. *Rev. Sci. Instrum.* **1985**, *56*, 373−376.

that tunes the crystal of the OPO. The wavelength of the OPO output is calibrated with a monochromator and a CCD detector. The total experimental uncertainty in the reported photon energies is ± 10 cm^{-1}.

The fragment ions are accelerated down a 1 m flight tube by a series of three stainless steel plates that have stainless steel mesh across an open center. Acceleration plate voltages are 3000 V, 2100 V, and ground, respectively, in order from furthest to nearest the detector. The flight tube is kept at 10^{-6} Torr using a Varian V300HT 6 in. air-cooled turbomolecular pump, and ions are detected using an 18 mm microchannel plate detector assembly. The detector assembly is fitted with two Galileo MCP 18B plates with a 10 μm channel diameter and a channel spacing of 12.5 μm. The ion current is processed using a computer-controlled RTD710 Tektronix 200 MHz dual-channel digitizer. A variable delay Stanford Research Systems model SR250 gated integrator and boxcar averager module is used for the wavelength dependence studies.

Photon emission spectra were obtained during photolysis of the title compound in an evacuated stainless steel six-way cross spectroscopy cell fitted with quartz windows. The output of the Nd:YAG pumped OPO is focused into the center of the chamber. The solid precursor is placed in the sample chamber and leaked into the deposition chamber with He as the carrier gas via a Teflon valve. The entire system is heated to the sublimation temperature of CpCoCOD using thermostated heating tape. The emitted light is collected by f/4 optics at right angles and directed into a Jobin-Yvon HR320 0.32 m single monochromator where it is dispersed by a 600 gr/mm holographic grating and detected by a EG&G Princeton Applied Research OMA3 UV-intensified diode array detector.

Results

1. Mass Spectroscopy of CpCoCOD. Mass spectra resulting from photofragmentation and ionization of CpCoCOD under excitation in the ultraviolet region and in the visible region from 410 to 500 nm are obtained. In general, the mass signal arising from the cobalt ion at *m*/*z* 59 is the dominant peak in the mass spectra obtained at all wavelengths studied. The parent ion, $CpCoCOD^+$ (*m*/*z* 232), the two monoligated species $Co(C_8H_9)^+$ and $CoCp^+$, and other metal-containing fragments such as $CODCo(C_3H_3)^+$, (C_5H_5)-$Co(C_5H_5)^+$, $Co(C_6H_6)^+$, $Co(C_3H_3)^+$, and $Co(C_2H_2)^+$ are observed in some spectra. The $Co(C_8H_9)^+$ fragment will be referred to as $CoCOD^+$ in this paper although three hydrogen atoms are lost and the exact structure is not known. The molecular fragments can undergo further fragmentation to yield the groups of peaks arising from the ligand fragments C_nH_n ($n = 1-8$). Optimization of the signals from the less intense molecular fragments upon excitation in the UV region leads to saturation of the signal from the dominant cobalt ions.

Mass spectra obtained after excitation in the UV and visible regions are shown in Figure 1. A list of the dominant peaks observed at each wavelength is presented in Table 1. Details about the mass spectra obtained at each of the wavelengths studied are presented in the following sections.

a. 266 nm Excitation. The mass spectra obtained at 266 nm are dominated by the signals arising from Co^+ (*m*/*z* 59) and the ligand fragments C_nH_n ($n = 1-8$) resulting from fragmentation of the Cp and COD ligands. A representative spectrum is shown in Figure 1a. Attempts to increase the relative intensity of the heavier fragments result in saturation of the Co^+ signal. The most surprising observation is the formation of the monoligated fragments $CoCp^+$ and $CoCOD^+$ in addition to the molecular ion. The ratio of $CoCp^+$ to the molecular ion is 2.5:1 while the ratio of $CoCp^+$ to $CoCOD^+$ is 7:1. Other metal-containing fragments such as $CpCo(C_6H_6)^+$, $Co(C_5H_5)^+$, $CpCo(C_4H_6)^+$, $Co(C_6H_6)^+$, $Co(C_3H_3)^+$, and $Co(C_2H_2)^+$ are observed. A magnification of the heavy mass region is shown in Figure 2.

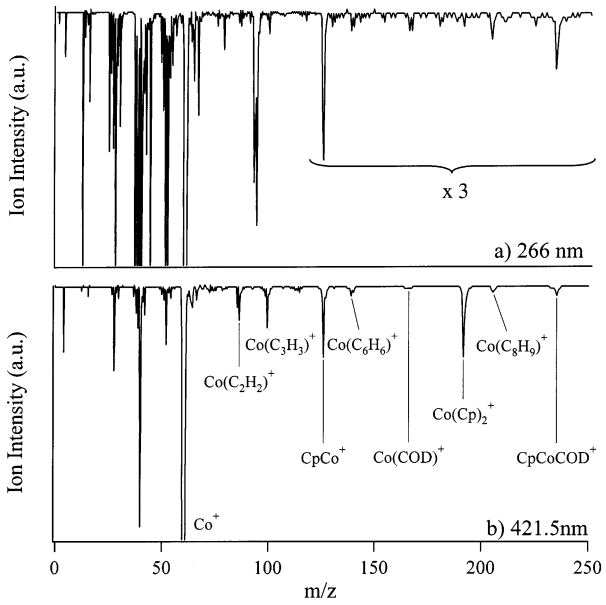

Figure 1. Mass spectra resulting from photolysis of CpCoCOD in (a) the UV region at 266 nm and (b) the visible region at 421.5 nm. The heavy mass region is magnified to emphasize the formation of the oxidized intact CpCoCOD molecule (*m*/*z* = 232) and the monoligated fragments $CoCp^+$ (*m*/*z* = 125) and $CoCOD^+$ (*m*/*z* = 164). The most intense peak at *m*/*z* = 59 corresponds to Co^+. A list of the observed peaks and their relative intensities is given in Table 1.

Table 1. Significant Mass Peaks Observed during Photoexcitation of (η^4-Cycloocta-1,5-diene)(η^5-cyclopentadienyl)cobalt at 266 and 421.5 nm

	relative intensity	
+ ion	266 nm	421.5 nm
C	**540**	5
CH_3	**160**	13
C_2H_3	**710**	120
C_3H_3	**860**	340
C_4H_3	**650**	82
Co	saturated	saturated
Cp	**190**	18
Co(CH)	trace	trace
C_6H_5	**69**	5
$Co(C_2H_2)$	26	**47**
C_7H_7	**390**	3
$Co(C_3H_3)$	40	**58**
COD	trace	trace
$Co(C_4H_6)$	2.9	2.6
CoCp	100	100
CoC_6H_6	**14**	13
CoCOD	**14**	2.6
$(C_5H_5)Co(C_4H_6)$	trace	trace
$(C_5H_5)Co(C_5H_5)$	11	**100**
$(C_5H_5)Co(C_6H_6)$	**20**	7.9
(C_3H_3)CoCOD	trace	trace
CpCoCOD	**40**	13

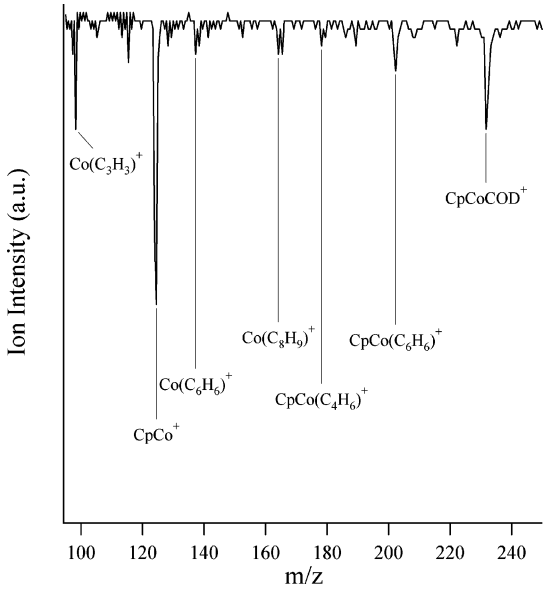

Figure 2. Mass spectrum illustrating the formation of coordinated ligand fragments resulting from fragmentation of a coordinated ligand with retention of coordinated fragments. CpCoCOD was photolyzed at 266 nm.

b. 308 and 355 nm Excitation. The mass spectra obtained at 308 and 355 nm are also dominated by signals arising from Co^+ and the ligand fragments, but the number of heavy ligand fragments and metal-containing fragments decreases dramatically and the number of smaller ligand fragments increases compared to those observed under 266 excitation. The only observed metal-containing fragment is $CoCp^+$, and no heavier fragments are observed. The $CoCp^+$ signal is weak and can barely be observed above the level of the noise in the mass spectrum observed at 355 nm when the Co^+ signal has saturated the detector as a result of efforts to maximize the intensity of the fragments in the heavier mass region. The peaks arising from the C_3H_n ($n = 1-9$) fragments are the most intense ligand fragment signals and are more intense relative to the metal-containing fragments than they are under 266 nm excitation. This type of fragmentation to yield the bare metal ion and fragments of the ligand is typical for metal-containing compounds.

c. Visible Excitation. The mass spectra obtained from excitation in the visible region between 410 and 500 nm are similar to those obtained at 266 nm. The mass spectrum obtained at 421.5 nm is shown in Figure 1b. The metal ion dominates the spectra, and metal-containing fragments are also observed. However, the relative intensities have changed significantly; the $CoCp^+$ to molecular ion ratio increases to 7.6:1 while the $CoCp^+$ to $CoCOD^+$ ratio increases to 37:1 upon changing the excitation wavelength. This relative increase in the amount of $CoCp^+$ to $CoCOD^+$ is observed throughout the visible region. At wavelengths longer than 460 nm, the mass spectrum is dominated by the Co^+ peak.

The mass spectrum in the heavy mass region obtained after UV excitation at 266 nm is compared to that obtained after visible excitation at 421.5 nm in Figure 1. Both spectra show the major metal-containing fragments and ligand fragments.

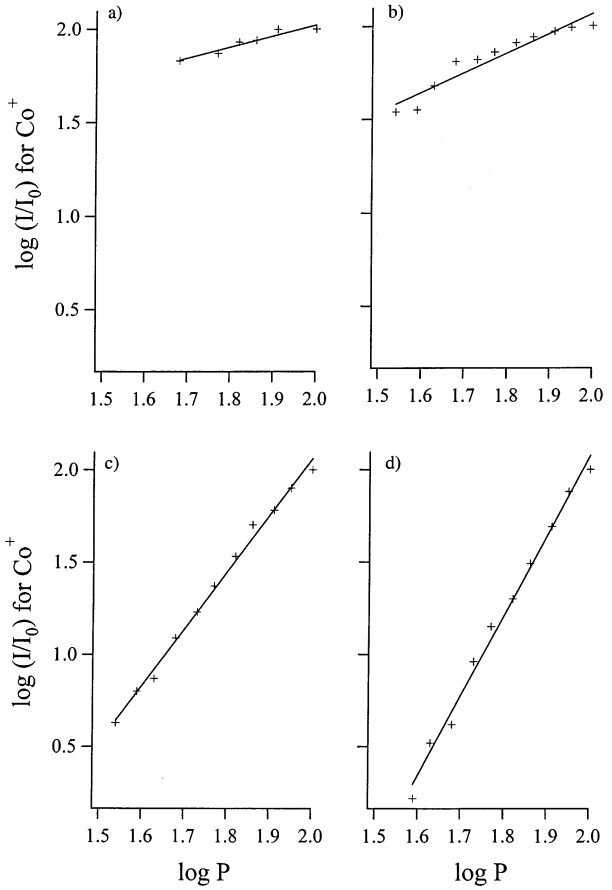

Figure 3. Power dependences for the production of Co^+ at (a) 266 nm, (b) 355 nm, (c) 420 nm, and (d) 483.6 nm.

The spectrum obtained in the UV is dominated by the Co^+ signal and the signals due to the free ligands and their fragments.

2. Fluence Dependence of Metal Ion Production. The effects of varying laser fluence on the overall yields of photofragmentation of CpCoCOD were studied at 266 nm, 355 nm, and several wavelengths in the visible region. log−log plots showing the power dependence of the cobalt ions at the wavelength regions studied are presented in Figure 3. As the energy of the exciting photons is increased, the overall photon dependence decreases. At 266 nm, there is an observed 0.6 photon dependence for the production of the cobalt ion. A three photon dependence is observed for formation of the cobalt ion in the visible region at 414.2, 420.4, and 432.2 nm. The photon dependence increases to 3.4 at 447.2 nm and 4.3 at 483.6 nm. Due to saturation effects, the actual number of photons involved may be larger.[47]

3. Wavelength Dependence of Fragmentation of CpCoCOD. a. Cobalt Ion. The wavelength dependence of the production of the $CoCp^+$ and Co^+ fragments was further investigated by monitoring the formation of these fragments as a function of the excitation wavelength. The variation of the intensities of the molecular ion and $CoCOD^+$ fragment could not be observed above the level of the noise. The

(47) Gedanken, A.; Robin, M. B.; Kuebler, N. A. *J. Phys. Chem.* **1982**, *86*, 4096−4107.

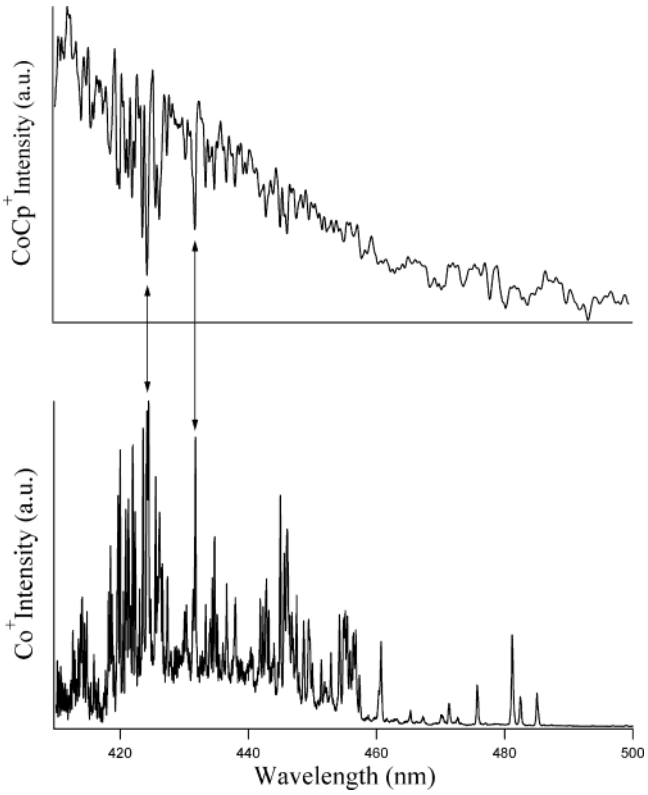

Figure 4. REMPI spectra obtained by monitoring the $CoCp^+$ fragment (top) and Co^+ (bottom). The dips in the top spectrum correspond to the peaks in the lower spectrum and arise from cobalt atomic absorption lines. The arrows point to two representative pairs of peaks and dips.

excitation spectra obtained while monitoring Co ion production in the 410−500 range are shown in Figure 4. The mass spectra obtained in this range show that Co^+ is the dominant photoproduct. The baseline in the Co^+ intensity begins to slowly increase starting at about 490 nm. There is a noticeable increase in the Co^+ intensity at about 460 nm before peaking at about 430 nm. The intensity of the Co^+ intensity reaches a minimum at 420 nm. The broad band contains many sharp peaks corresponding to Co atom resonances. The assignment of the sharp peaks as Co atom resonances was confirmed by comparing the spectrum obtained by monitoring Co^+ production from CpCoCOD to the spectrum obtained by monitoring Co^+ production from $(PhC{\equiv}CPh)Co_2(CO)_6$. The two spectra contain the same sharp peaks. The most intense Co atom resonances occur at 424.0 and 432.0 nm and are within the experimental uncertainty of reported cobalt atom resonances due to the $^6F_{11/12}{}^0 \rightarrow {}^4F_{9/2}$ and $^2F_{7/2}{}^0 \rightarrow {}^2D_{5/2}$ transitions.[48]

b. $CoCp^+$. The excitation spectrum obtained while monitoring $CoCp^+$ production in the 410−500 nm range is shown at the top of Figure 4. The spectrum is much less intense than that for Co^+, and many of the interesting features are lost in the noise. This is probably due to the fact that the signal arising from $CoCp^+$ is much less intense than that arising from Co^+. The most noticeable feature of the spectrum is the generally broad band that begins to show an increase in intensity starting at around 490 nm. The increase in intensity of the $CoCp^+$ excitation closely follows that of the Co^+ ion spectra but continues to increase to shorter wavelengths (higher energies). However, the presence of peaks on the underlying broad bands is now replaced with sharp losses of intensity at energies corresponding to Co atom resonances. It is difficult to observe these "dips" in the $CoCp^+$ spectrum, but the double-headed arrows at 424 and 432 nm in Figure 4 label the most obvious occurrences.

4. Photoemission from Cobalt Atoms. The gas-phase emission spectrum obtained by exciting CpCoCOD in the UV in the presence of He carrier gas is dominated by a broad band from 350 to 525 nm. Four sharp peaks are observed at 347.8, 353.8, 391.7, and 402.0 nm. No other sharp features are observed in the region studied. The sharp peaks arise from known atomic cobalt transitions.[48] There are a plethora of cobalt atom resonances at wavelengths greater than 400 nm, but they do not have reported intensities comparable to the transitions observed and only appear as a broad unresolved feature in our spectra. No molecular emission or emission due to free ligands is observed.

Discussion

The gas-phase photofragmentation reactions of CpCoCOD exhibit three surprising features that are uncommon in the reactions of organometallic compounds in the gas phase. First, significant amounts of the intact cation are formed. Usually fragmentation of organometallics occurs before ionization; this rule of thumb is explained by the relatively weak metal−ligand bond strengths (in comparison to those of organic molecules where ionization frequently occurs before fragmentation).[47] Second, in the mixed-ligand CpCoCOD compound, the relative amounts of Cp and COD photodissociation are wavelength dependent. Third, fragmentation of the ligands occurs while the ligands are still coordinated giving rise to photoproducts containing coordinated fragments of the original ligand. Again, breaking several carbon−carbon bonds with retention of weaker metal−ligand bonds is unexpected. These features are discussed below.

1. Photoionization of the CpCoCOD Molecule. The mass spectra obtained by exciting with 266 nm light and with light in the visible region from 410 to 500 nm are not characteristic of those previously reported for related metallocenes or other metal-containing compounds. Photoionization of CpCoCOD to form the intact molecular ion at *m*/*z* 232 is observed with both ultraviolet and visible excitation in contrast to the extensive fragmentation that is usually observed from organometallic compounds. The intensity of the molecular ion peak relative to that of the most intense fragment peak (from $CoCp^+$) varies from 0.4:1 to 0.13:1 when the excitation wavelength is changed from 266 to 421.5 nm. Within the visible region, this ratio varies from 0.4:1 to 0.11:1. In the spectra with the best signal-to-noise ratio, a broadening of the molecular ion peak toward smaller *m*/*z* values is observed. This broadening is caused by the added contribution to the molecular ion signal from the species $CpCo(C_8H_{10})^+$ in which the COD ligand has lost two protons. No contribution from $CpCo(C_8H_{11})^+$ is observed in the

(48) Meggers, W. F.; Corliss, C. H.; Scribner, B. F. *Tables of Spectral-Line Intensities*; National Bureau of Standards: Washington, DC, 1975.

spectrum. Although the molecular ion is observed at shorter wavelengths in the visible region, it is not observed at the longer wavelengths, possibly to decreased laser fluence and absorption cross section of the molecule at the longer wavelengths.

The vertical ionization energy of CpCoCOD is 6.96 eV,[49] corresponding to about 1.5 photons at 266 nm (4.67 eV/photon) and almost 2.5 photons in the visible region between 410 and 500 nm (3.0−2.5 eV/photon). The average bond disruption enthalpy for cobaltocene is only 1.58 eV.[50] This value was calculated for the homolytic loss of a Cp ligand $Cp2M(g) \rightarrow 2Cp\bullet(g) + M^0(g)$. Assuming that the relative M−Cp strengths are comparable in cobaltocene and CpCoCOD, it is surprising that the absorption of multiple photons results in the photoionization of the intact molecule prior to ligand loss rather than metal−ligand bond cleavage.

As mentioned previously, photoionization studies of metal-containing compounds have mainly resulted in the observation of the metal ion and only trace amounts of the molecular ion. Recently, however, it was reported that photoionization of the intact chromocene molecule dominates fragmentation to the bare metal ion at some wavelengths.[36] In the case of cobalt, the intensity of the $CpCoCOD^+$ molecular ion never approaches that of the cobalt ion, but the observation of the photoionized intact molecule shows that ionization prior to fragmentation does occur in these types of metal-containing compounds.

2. Wavelength Dependence of the Photodissociation of the Cp and COD Ligands. The monoligated fragments $CoCp^+$ and $CoCOD^+$ result from the loss of the COD or the Cp ligand, respectively. (The fragment referred to as $CoCOD^+$ (*m*/*z* 164) corresponds to the $Co(C_8H_9)^+$ fragment and does not contain the intact C_8H_{12} COD ligand.) It is possible, but very unlikely, that this peak could contain contributions from the $(C_5H_5)Co(C_3H_3)^+$ fragment; the internal rearrangements that occur in the COD ligand while still associated with the metal center will be discussed later. The $CoCp^+$ (*m*/*z* 125) signal does not contain observable contributions from deprotonated fragments such as $(C_5H_4)Co^+$.

The loss of the individual COD and Cp ligands has a dependence on the wavelength of excitation. Mass spectra obtained in the visible region between 410 and 460 nm differ from those obtained in the UV with respect to the relative ratios of the photofragments. Generally, the metal-containing molecular fragments in which the cyclooctadiene ligand is still attached, such as $CpCoCOD^+$, $(C_3H_3)CoCOD^+$, and $CoCOD^+$, are more intense under UV excitation while those without the cyclooctadiene ligand such as $CoCp^+$ are more intense under visible excitation. Both the total amounts and the relative amounts of the molecular fragments change. The $CoCp^+$ to molecular ion ratio increases from 2.5:1 to 7.6:1 while the $CoCp^+$:$CoCOD^+$ ratio increases from 7:1 to 37:1 in going from 266 nm excitation to visible wavelength excitation.

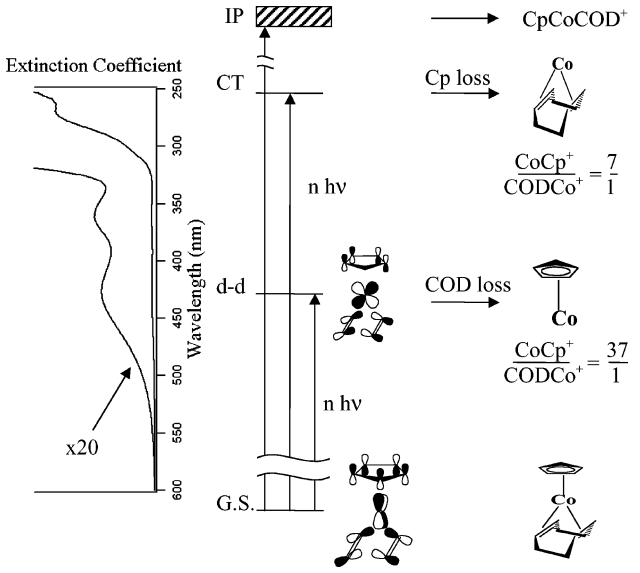

Figure 5. Schematic energy level diagram illustrating the states initially populated and the resulting fragmentation reactions. The electronic absorption spectrum is shown on the left, and the d−d and charge-transfer excited states that correspond to the transitions are shown to its right. The change in the ratios of intensities of the $CoCp^+$/$CODCo^+$ fragments are given immediately under the sketches of the fragments.

These results suggest that although either the Cp or the COD ligand can be lost independently leading to formation of the corresponding molecular fragment, the *relative* amount of loss has a significant wavelength dependence. For example, the COD ligand is always lost to a greater extent than the Cp ligand at all wavelengths studied, but the relative amount of loss is greatest under visible excitation. A possible explanation for the favored loss of COD at all excitation wavelengths is based on the relative bond strengths: the Co−alkene bond is weaker than the Co−Cp bond and is most easily broken.

The change in the *ratio* of Cp vs COD ligand loss can be explained in terms of the molecular orbitals initially populated as shown in Figure 5. The absorption spectrum of CpCoCOD[51] consists of two d−d bands at 426 and 361 nm and two charge-transfer bands at 303 and 270 nm.[49] The mass spectra result from excitation of the lowest and highest energy absorption bands at 426 and 270 nm. Absorption in the visible corresponds to a d_{xz} to d_{yz} transition[51] that causes a decreased bonding interaction between the CoCp fragment and the COD ligand (Figure 5). (The d_{xz} and d_{yz} orbitals are labeled according to the coordinate system with the *x*-axis defined as the axis parallel to both the cyclopentadienyl ring and the carbon−carbon double bonds of the cyclooctadienyl ring while the *y*-axis is defined as the axis parallel to the Cp ring and perpendicular to the COD double bonds.) Excitation at 266 nm involves the highest energy CT band and the removal of an electron from a metal−ligand bonding orbital to a ligand-centered orbital that is not involved in bonding to the metal. The greater amount of COD ligand loss using visible excitation may thus be a result of the greater metal−COD bond weakening that occurs in the initially populated d−d excited state.

(49) Green, J. C.; Powell, P.; van Tilborg, J. E. *Organometallics* **1984**, *3*, 211−217.
(50) Ryan, M. F.; Richardson, D. E.; Lichtenberger, D. L.; Gruhn, N. E. *Organometallics* **1994**, *13*, 1190−1199.
(51) Bailey, S. E.; Cohan, J. S.; Zink, J. I. *J. Phys. Chem.* **2000**.

An alternative explanation for the wavelength dependence, suggested by a reviewer, is based on energy deposition in the molecule. Longer wavelengths may be more likely to create photoexcited species near the threshold for ligand loss and would favor the lower energy channel. The mass spectra shown in Figure 1 are consistent with this explanation; the multiphoton fragmentation is less complete at visible wavelengths. Because the lower energy excitation populates metal−ligand antibonding orbitals which also favor the lower energy ligand loss channel as discussed above, the data do not differentiate between the possible explanations for this molecule.

3. REMPI Spectra and the Wavelength Dependence of the Formation of $CoCp^+$ and Co^+. To further characterize the wavelength dependence of ligand photolabilization, the mass selected REMPI spectra were obtained by monitoring the two most intense fragments, $CoCp^+$ and Co^+. (In the REMPI experiment, the intensity of the fragment is measured as a function of wavelength.) The spectra are shown in Figure 4.

a. REMPI Spectrum of $CoCp^+$. The excitation spectrum obtained by monitoring the variation in intensity of the $CoCp^+$ fragment as a function of the excitation wavelength is shown in Figure 4 (top). The spectrum shows an onset at about 470 nm. The intensity constantly increases and reaches its maximum at the end of the scanning range of the instrument. The band contains a large number of sharp features that are losses (rather than gains) in intensity.

b. REMPI Spectrum of Co^+. The excitation spectra obtained by monitoring the Co^+ intensity as a function of the excitation wavelength is shown in Figure 4 (bottom). Weak features are observed between 500 and 530 nm. The onset of the broad band at 470 nm is similar to that observed in the spectrum obtained by monitoring $CoCp^+$. The broad band contains many superimposed sharp features corresponding to gains in intensity.

The onset of the excitation spectra occurs at about the same energy as the onset of the solution phase absorption of the molecule. This similarity suggests that the absorption of the first photon involves the same excited state as that involved in the lowest energy solution absorption band. As discussed in the previous section, the lowest energy state arises from a d−d transition that weakens the Co−COD bond.

c. Cobalt Atom Resonances. The most significant features of the action spectra monitoring Co^+ are the sharp lines that dominate the broad underlying structure. These sharp lines are assigned to cobalt atomic absorption lines. To verify experimentally that these lines are caused by electronic transitions in cobalt atoms, the REMPI spectrum of a different organometallic cobalt compound, $(PhC{\equiv}CPh)Co_2(CO)_6$, was measured. The sharp lines that were observed from this compound coincide with the sharp features observed in the spectrum from CpCoCOD. The gas-phase luminescence spectrum obtained form CpCoCOD contains luminescence bands from neutral cobalt atoms and provides independent verification that cobalt atoms are present.

An interesting result can be seen when comparing the REMPI spectrum monitoring the Co^+ to that obtained while monitoring the $CoCp^+$ ion. The spectrum obtained monitoring the $CoCp^+$ fragment contains sharp *losses* of intensity at wavelengths corresponding to the sharp peaks in the Co^+ spectrum that result from the Co atom resonances. This process has been observed previously in our laboratory with other metals[35,36,40,52] and can possibly be explained by (a) inner filter effects that decrease the amount of photons available for $CoCp^+$ ionization after the strong absorbance due to Co resonances or (b) neutralization of the $CoCp^+$ fragments by electrons released from cobalt atoms upon ionization.[36]

4. Fragmentation of Coordinated Ligands. The intact molecule CpCoCOD and the monoligated molecules $CoCp^+$ and $CoCOD^+$ undergo fragmentation of the remaining coordinated ligand resulting in smaller metal-containing fragments. The precursor molecular ion can lose either the intact Cp ligand or the intact COD ligand to form a monoligated compound as discussed previously. Each of the monoligated molecules undergoes fragmentation of the coordinated ligand to produce new coordinated ligands not present in the parent molecule such as $Co(C_6H_6)^+$, $Co(C_4H_6)^+$, $Co(C_3H_3)^+$, $Co(C_2H_2)^+$, and $Co(CH)^+$. In addition, the COD ligand on the precursor molecule can undergo fragmentation while the Cp ligand is still attached to produce $(C_5H_5)Co(C_6H_6)^+$, $(C_5H_5)Co(C_5H_5)^+$, and $(C_5H_5)Co(C_4H_6)^+$. The identities of the fragments and their intensities relative to that of $CoCp^+$ (the most intense metal-containing molecular ion) are listed in Table 1. The fragments' peaks are in some cases broadened due to contributions from ligands with various degrees of protonation; the listed fragments constitute the major component of each peak. A sequential pattern of fragments is not a common photodecomposition pathway for these types of compounds. These processes are discussed further in the following sections.

a. Fragmentation after COD Loss. Upon photoexcitation, the most important ligand loss process produces $CoCp^+$ from loss of the COD ligand. Surprisingly, the coordinated C_5H_5 can undergo fragmentation while still coordinated to the cobalt, yielding smaller compounds such as $Co(CH)^+$, $Co(C_2H_2)^+$, $Co(C_3H_3)^+$, and $Co(C_4H_6)^+$ (Figure 6). The path to formation of these small fragments from the breakup of CoCp may occur via reduced hapticity of the Cp ligand. For example, excitation could produce an η^3 type coordination between the Cp ligand and the metal center in which the ring has slipped from the initial η^5 type coordination.[53] The cyclopentadienyl ligand with allyl type coordination could lose an ethylene leaving behind an η^3 allyl group bound to the metal. The three-carbon allyl-type ligand is the most abundant of these small fragments; the two-carbon ethylene- or acetylene-type ligand is the next most intense, and the one-carbon carbyne type ligand and the four-carbon coordinated fragment are produced in only trace amounts (Table 1).

b. Fragmentation after Cp Loss. After the Cp ligand is photodissociated, the coordinated COD ligand can undergo

(52) Muraoka, P.; Byun, D.; Zink, J. I. *J. Am. Chem. Soc.* **2000**, *122*, 5670.
(53) Wakatsuki, Y.; Yamazaki, H.; Kobayashi, T.; Sugawara, Y. *Organometallics* **1987**, *6*, 1191−1196.

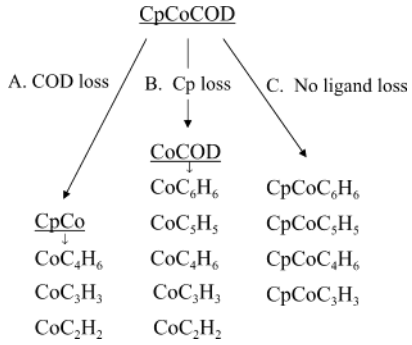

Figure 6. Fragmentation pathways of the Cp and COD ligands while they are coordinated to cobalt. (A) Loss of the COD ligand leads to formation of the CpCo fragment; further fragmentation of the coordinated Cp ligand leads to the species shown. (B) Loss of the Cp ligand leads to formation of the CoCOD fragment; further fragmentation of the coordinated COD ligand leads to the species shown. (C) Fragmentation of coordinated COD bonded to the intact compound leads to the species shown. Cobaltocene ($Co(Cp)_2 = CpCoC_5H_5$) is the dominant product in this fragmentation pathway.

fragmentation to yield smaller metal-containing molecular ions. (In fact, the intact C_8H_{12} is not observed after Cp dissociation; the major fragment containing the coordinated COD ligand is $Co(C_8H_9)^+$.) The most surprising small fragment that is formed from CoCOD is $Co(C_6H_6)^+$. The six-carbon $Co(C_6H_6)^+$ can only result from fragmentation of the eight-carbon $CoCOD^+$ and probably involves loss of ethylene. It is likely that some of the five-carbon $Co(C_5H_5)^+$ results from loss of allene, but the majority of this fragment probably originates from COD dissociation. The heaviest fragment, $Co(C_7H_7)^+$, is not observed in our studies. All of the possible smaller fragments are produced including $Co(C_4H_6)^+$, $Co(C_3H_3)^+$, $Co(C_2H_2)^+$, and $Co(CH)^+$. However, these fragments could also originate from fragmentation of coordinated Cp as discussed above.

The formation of metal-containing fragments with ligands containing less than four carbons is probably a result of fragmentation after COD ligand loss. The metal−ligand bond strength is smallest for the cobalt−COD ligand, and thus, COD dissociation occurs readily. As discussed in section 2, the $CoCp^+$ ion is the dominant metal-containing fragment at all wavelengths. There is precedent for formation of coordinated C_2 and C_3 fragments from coordinated Cp. The photofragmentation of chromocence, $Cr(Cp)_2$, produced $Cr(C_2)$ $Cr(C_3)$, and $CpCr(C_3)$ fragments.[36]

c. Fragmentation of COD without Loss of the Cp Ligand. When both the Cp and COD ligands remain coordinated to the metal center, only the COD ligand undergoes fragmentation. The $CpCo(C_6H_6)^+$, $CpCo(C_5H_5)^+$, and $CpCo(C_4H_6)^+$ fragments are observed (Figure 6). The formation of $CpCo(C_6H_6)^+$ is the strongest proof that the COD ligand coordinated to the intact parent molecule undergoes fragmentation while coordinated and leaves behind coordinated fragments. (No $CpCoC_7^+$ species is observed.) The fragments with a total carbon atom count of eight or less could originate from fragmentation of CoCOD as discussed above. The most intense of these peaks, the one at *m*/*z* 189 indicating the formation of cobaltocene, (C_5H_5)-$Co(C_5H_5)^+$, could be a result of a chemical reaction in the sample chamber as CpCoCOD is heated prior to being expelled through the pulsed nozzle assembly, but the presence of the intact molecular ion $CpCoCOD^+$ in the spectrum suggests that this process is minimal. The most likely possibility is that it is a photoproduct resulting from the fragmentation of the coordinated cyclooctadienyl ligand of the intact molecule by expulsion of a C_3 fragment.

Summary

The photofragmentation of CpCoCOD in the gas phase is wavelength dependent. The peak due to Co^+ is the largest observed mass signal at all wavelengths of excitation studied, but peaks arising from the parent ion as well as other metal-containing molecular fragments are observed. Photoexcitation at 266 nm and in the visible region results in the surprising formation of $CoCp^+$ and $CoCOD^+$ in addition to the molecular ion. Metal-containing fragments such as $CpCo(C_6H_6)^+$, $Co(C_5H_5)^+$, $CpCo(C_4H_6)^+$, $Co(C_6H_6)^+$, $Co(C_3H_3)^+$, and $Co(C_2H_2)^+$ are also observed. Intramolecular fragmentation of the monoligated fragments $CoCp^+$ and $CoCOD^+$ as well as COD fragmentation without loss of the Cp ligand results in the formation of new coordinated ligands.

The appearance ratios of these larger fragments are highly dependent on the wavelength of excitation and initially accessed excited state. The relative ratios of non-COD-containing fragments to COD-containing fragments increases as the wavelength is changed from excitation of the charge-transfer band in the UV to excitation of the lowest energy d−d band in the visible. The $CoCp^+$ to molecular ion ratio increases from 2.5:1 to 7.6:1 as the excitation is changed from 266 to 421.5 nm while the $CoCp^+$ to $CoCOD^+$ ratio increases from 7:1 to 37:1. Within the visible region, the $CoCp^+$ to molecular ion ratio varies from 2.5:1 to 9.1:1. This wavelength dependence can be explained in terms of bonding changes in the initially populated excited state and is attributed to an overall decrease in the bonding interaction between the CoCp fragment and the COD ligand. The REMPI spectrum of Co^+ shows sharp peaks at wavelengths at which sharp losses of intensity are observed in the REMPI spectrum obtained monitoring $CoCp^+$. The sharp peaks are assigned as Co atom transitions while the sharp losses in intensity can be attributed to inner filter effects or electron capture mechanisms.

Acknowledgment. This work was made possible by a grant from the National Science Foundation (CHE 0102623). We thank Dr. Alf Bacher and Andy Cerin for assistance with the synthesis of CpCoCOD.

IC0300518